Journal of Cellular Biochemistry 93:774–787 (2004)

In Vivo Activated Caspase-3 Cleaves PARP-1 in Rat Liver After Administration of the Hepatocarcinogen *N*-Nitrosomorpholine (NNM) Generating the 85 kDa Fragment

Józefa Węsierska-Gądek,* Marieta Gueorguieva, Jacek Wojciechowski, and Slavica Tudzarova-Trajkovska

Cell Cycle Regulation Group, Institute of Cancer Research, Medical University of Vienna, A-1090 Vienna, Austria

Abstract We reported previously that treatment of rats with the hepatocarcinogen *N*-nitrosomorpholine (NNM) caused severe hepatotoxicity associated with apoptosis of hepatocytes beginning 12 h after administration of NNM. We observed that poly(ADP-ribose) polymerase 1 (PARP-1), one of the major nuclear targets for caspases, was proteolytically degraded generating primarily 64 and 54 kDa fragments. Interestingly, at 20, 30, and 40 h post-treatment a 85 kDa cleavage product of PARP-1 resembling that generated by caspase-3 appeared additionally in hepatocytes. More detailed analysis performed in the present study revealed that the 85 kDa fragment of PARP-1 was generated in the liver in 10 of 17 (60%) animals examined between 20 and 40 h after NNM administration. The caspase-3 generated 85 kDa fragment was detected solely in hepatocytes undergoing apoptosis as evidenced by immunostaining performed with the antibody recognizing exclusively PARP-1 cleaved at position 214/215. The appearance of the 85 kDa fragment of PARP-1 in the liver nuclei coincided temporally with an significant increase of caspase-3 activity in hepatocytes. In contrast, in testis samples obtained from the same animals, no changes characteristic for apoptosis such as induction of caspases activity or degradation of nuclear PARP-1 could be detected. Our results evidence unequivocally that PARP-1 in liver is not resistant to caspases and can be processed in vivo by activated caspase-3 producing the p85 kDa fragment. Moreover, the caspase-3 induced PARP-1 fragmentation coinciding with the increase of caspase-3 activity was detected solely in the target organ and exclusively in hepatocytes undergoing apoptosis. Considering the fact that the caspase-3 mediated PARP-1 cleavage occurred only in 60% of animals tested between 20 and 40 h, it becomes obvious that the cellular response in vivo to the same trigger(s) strongly varies and may depend on a variety of intrinsic factors. It remains to elucidate which additional factors may be involved in the modulation of cellular response to the strong insults thereby activating different pathways and generating distinct outcomes. J. Cell. Biochem. 93: 774–787, 2004.

Key words: PARP-1 cleavage; caspase-3 activation; cytochrome C release; AIF release

N-nitrosomorpholine (NNM) is a highly cytotoxic and genotoxic compound [Stewart et al., 1975; Moore et al., 1982; Enzmann and Bannasch, 1987; Weber and Bannasch, 1994] generating different types of DNA damage [Brambilla et al., 1987]. After genotoxic shock cells induce a defence response allowing to repair the DNA lesions or to eliminate the severely damaged cells by apoptosis Tamm et al. [2001]. The accurate regulation of the defence strategy reduces the risks of neoplastic transformation [Thorgeirsson et al., 1998].

Abbreviations used: AIF, apoptosis inducing factor; CP, cisplatin; DAPI, 4,6-diamidino-2-phenylindole; DOX, doxorubicin; HRP, horseradish peroxidase; NNM, *N*-nitrosomorpholine; MCM-7, minichromosome maintenance-7; PARP-1, poly(ADP-ribose)polymerase-1; PBS, phosphate-buffered saline; PCNA, proliferating-cell nuclear antigen; PMSF, phenylmethylsulfonyl fluoride; PNS, post-nuclear supernatant; PVDF, polyvinylidene difluoride; TdT, terminal deoxynucleotidyl transferase; ts, temperature-sensitive; TUNEL, TdT-dUTP-nick-end-labeling; VP-16, etoposide; WCL, whole cell lysate; wt, wild-type.

Grant sponsor: Jubiläumsfonds der Österreichischen Nationalbank; Grant number: 10340.

*Correspondence to: Dr. Józefa Węsierska-Gądek, Cell Cycle Regulation Group, Institute of Cancer Research, Borschkegasse 8 a, A-1090 Vienna, Austria.
E-mail: Jozefa.Gadek-Wesierski@meduniwien.ac.at

Received 10 February 2004; Accepted 20 April 2004
DOI 10.1002/jcb.20181

In normal rat liver in vivo the oral application of nitrosamine NNM triggered apoptosis which was apparently unrelated to p53 [Wesierska-Gadek et al., 1999]. The induction of apoptosis preceded the activation of p53 protein and showed a different spatial distribution than the upregulated p53 protein [Wesierska-Gadek et al., 1999]. Recently, we observed a strong induction of p73 expression in rat liver after a single application of NNM [Tudzarova-Trajkovska and Wesierska-Gadek, 2003]. The p73 increase preceded the onset of apoptosis. Several hepatocyte nuclei in the early stage of apoptosis expressed p73 protein as evidenced by immunostaining. These results strongly suggest that p73 can serve as inducer of apoptosis in the liver following genotoxic injury.

Interestingly, we observed that during the execution of apoptosis in the liver of NNM treated rats different patterns of degradation of nuclear targets were generated. Poly(ADP-ribose) polymerase 1 (PARP-1), one of the major nuclear targets for caspases, was proteolytically degraded generating primarily 64 and 54 kDa fragments. Interestingly, between 20 and 40 h post-treatment, a 85 kDa canonical cleavage product of PARP-1 additionally appeared in the liver but not in testis. More detailed analysis revealed that the 85 kDa fragment of PARP-1 was generated in the liver of 10 out of 17 animals (60%).

The 85 kDa trunctated PARP-1 which is known to be generated by activated caspase-3 was detected solely in hepatocytes undergoing apoptosis as evidenced by immunostaining performed with the antibody recognizing selectively PARP-1 cleaved at position 214/215, representing the caspase-3 recognition motif. The appearance of the 85 kDa fragment of PARP-1 in the liver nuclei coincided temporally with a significant increase of caspase-3 activity. Comparison of the kinetics of the release of apoptosis inducing factor (AIF) from liver mitochondria and the activation of effector caspases shows a close temporal correlation. However, in testis samples obtained from the same animals no changes characteristic for apoptosis could be detected.

There are contradictory data on the in vivo PARP-1 processing by caspases. It has been reported previously that PARP-1 in the liver is resistant to cleavage by caspases [Jones et al., 1999]. Our results evidence unequivocally that PARP-1 in the liver can be processed by activated caspase-3 to the p85 kDa fragment in vivo. However, cellular response in vivo to the same trigger strongly varies because the caspase-3 generated PARP-1 cleavage occurred only in 60% of tested animals. It remains to elucidate which additional factors may be involved in the modulation of cellular response to the strong insults thereby activating different pathways and generating distinct outcomes.

MATERIALS AND METHODS

Animals and Treatment

Two independent animal experiments were performed. Three to five weeks old male SPF Wistar rats were used in our studies. NNM was dissolved in phosphate-buffered saline (PBS). Rats (three animals per time point) were given a single dose of 250 mg NNM/kg body weight by oral gavage between 8 p.m. and 9 p.m. when the wave of hepatic DNA synthesis was at its peak, as described previously in detail [Wesierska-Gadek et al., 1999]. Controls were treated with solvent (10 ml/kg). In the first experiment the rats were killed under carbon dioxide anoxia by decapitation and exsanguinated 6, 12, 20, 40, 60, 84, and 156 h after NNM administration. In the second experimental series the experimental group at 20 h post-treatment was extended to five animals and additionally animals with shorter intervals after NNM administration were analyzed. The animal experiments were performed in the facilities of the Experimental Animal Laboratory of the Vienna Medical University according to the Austrian guidelines for animal care and treatment.

Cells and Treatment

Human cervix carcinoma HeLa S_3 and HTB-31 cell lines obtained from the American Association for Cell Culture (AACT) were used. In some experiments cells were treated with 20 μM cisplatin (CP), 1 μM doxorubicin (DOX), or etoposide (VP-16) for indicated periods of time. Ewing sarcoma cells expressing temperature-sensitive (ts) human $p53^{138val}$ mutant were shifted to 32°C for 6 h [Kovar et al., 2000].

Antibodies

We used in this study different anti-PARP-1 antibodies and antibodies against another antigens. A monoclonal mouse anti-PARP-1 (C-2-10) antibody, a monoclonal mouse antibody against minichromosome maintenance-7 protein (MCM-7) (DCS141.2) and a monoclonal mouse anti-proliferating-cell nuclear antigen

(PCNA) antibody (PC-10) were from Oncogene Research Products (Cambridge, MA). A monoclonal antibody against AIF (clone E-1) was from Santa Cruz, Inc. (Santa Cruz, CA). Polyclonal anti-caspase-3 antibodies were from Upstate Biotechnology (Lake Placid, NY). An anti-p85 polyclonal rabbit antibody (Promega, Madison, WI) was additionally used. A monoclonal mouse anti-cytochrome C antibody (7H8.2C12) was obtained from BD PharMingen (San Diego, CA). A polyclonal antibodies against intact PARP-1 was from NeoMarker, (Fermont, CA). A monoclonal anti-ran antibodies (clone 20) were from Transduction Laboratories (Lexington, KY) and anti-actin antibodies (clone 4) were from ICN Biochemicals (Aurora, OH). Appropriate secondary antibodies linked to horseradish peroxidase (HRP) were from Pierce (Rockford, IL).

Histology

Tissue paraffin sections (3–4 μm thick) were prepared from liver slices fixed in 4% buffered formalin immediately after isolation of organs. Liver sections were stained with polyclonal antibodies against intact PARP-1 (NeoMarker) or with antibodies recognizing solely caspase-3 cleaved PARP-1 (214/215) (Promega) according to the manufacturer's protocol and then counterstained with hematoxylin and eosin (H&E) for evaluation of the hepatocyte morphology. Immune complexes were detected after incubation with appropriate secondary antibodies coupled to HRP using 3,3′-diaminobenzidine tetrahydrochloride and H_2O_2 as a substrate as described previously [Tudzarova-Trajkovska and Wesierska-Gadek, 2003].

Determination of Apoptosis in Individual Cells

To detect chromatin fragmentation in individual cells, we stained the tissue paraffin sections by Hoechst 33258. To assess DNA fragmentation in individual cells we performed the TdT-dUTP-nick-end-labeling (TUNEL) enzymatic labeling assay in situ as previously described [Tudzarova-Trajkovska and Wesierska-Gadek, 2003]. This widely used method is based on the enzymatic labeling of DNA strand breaks (free 3′-OH termini) with modified nucleotides (e.g., fluorescein-12-dUTP) using exogenous terminal deoxynucleotidyl transferase (TdT). Tissue paraffin sections (3–4 μm) were dewaxed and rehydrated and then processed for labeling using the DeadEnd Fluorometric TUNEL Kit (Promega) according to the procedure recommended by manufacturer's. Samples were counterstained with propidium iodide at a final concentration of 1 μg/ml and immediately evaluated. The number of hepatocytes undergoing apoptosis was determined by TUNEL assay combined with propidium iodide staining. The evaluation of the nuclear morphology allowed to discriminate between hepatocytes undergoing apoptosis and necrosis. At least 4,000 hepatocytes were scored from each sample.

Isolation of Nuclei and Cytosolic Fraction From Rat Liver and Testes

To avoid proteolytic degradation of proteins, all isolation steps were performed at +4°C in the presence of the protease inhibitors phenylmethylsulfonyl fluoride (PMSF) and Pefabloc at a final concentration of 1 mM and 100 μM, respectively. Nuclei were isolated by the method of Tata [1974]. Post-nuclear supernatant (PNS) was ultracentrifuged as previously described by Fiskum et al. [2000] yielding a pellet containing mitochondria and a supernatant designated as cytosol.

Determination of Protein Content

Aliquots of isolated nuclei were dissolved in non-reduced SDS-sample buffer. Protein concentration in isolated nuclei, cell lysates, and cytosol samples was determined by the DC assay (Bio-Rad Laboratories, Richmond, CA) using bovine serum albumin as standard.

Determination of Caspase-3/7 Activity

The activity of both caspases was determined using the APO-ONE Homogenous Caspase-3/7 Assay (Promega). This test uses the caspase-3/7 substrate rhodamine 110, bis-(*N*-CBZ-L-aspartyl-L-glutamyl-L-valyl-L-aspartic acid amide (Z-DEVD-R100). This compound exists as a pro-fluorescent substrate prior to the assay. Upon cleavage and removal of the DEVD peptide by caspase-3/7 activity and excitation at 499 nm, the rhodamine 110 leaving group becomes intensely fluorescent. Equal amounts of cytosolic proteins prepared from control and NNM treated rats were diluted with sucrose buffer to a final volume of 50 μl. Then an equal volume of caspase substrate was added and samples were incubated at 37°C for 2, 4, and 20 h. The fluorescence was measured at 485 nm. Sucrose buffer was used as a blank. "no-cell

background" values after 20 h were about 10,000 cpm.

Immunoblotting

Proteins dissolved in reduced SDS sample buffer were loaded on SDS polyacrylamide slab gels, electrophoretically separated, and transferred onto polyvinylidene difluoride (PVDF) membrane (Amersham International, Little Chalfont, England). Equal loading of proteins and appropriate electroblotting was confirmed by Ponceau S staining. The protein loading was additionally proved by sequential incubation of the blots with anti-ran or anti-actin antibodies. Ran is a highly conserved GTPase that is ubiquitously expressed. At steady state, ran is located in nucleus and in the cytoplasm. Immunodetection of antigens was performed with specific primary antibodies [Wesierska-Gadek et al., 1998]. The immune complexes were detected autoradiographically using appropriate HRP-linked secondary antibodies and enhanced chemiluminescence detection reagent ECL+ (Amersham International) using LS film (Eastman Kodak Co., Rochester, NY).

Statistical Analysis

Statistical analysis was performed by the ANOVA test followed by Dunnett's Multiple Comparison Test (all treatment groups vs. control).

RESULTS

Evaluation of Apoptosis

Treatment of rats by NNM was highly cytotoxic. Within the first days after administration of a single NNM dose sacrificed rats displayed considerable loss of liver tissue. At 20 h after NNM administration liver mass was reduced by about 40% and at 40 h by 60% (Table I). To determine the induction of apoptosis in response to treatment with the hepatocarcinogen NNM, a few independent methods were used. First, NNM-induced fragmentation of chromatin in hepatocytes was evaluated in liver tissue sections stained with Hoechst 33258. As shown in Figure 1, in specimens prepared from liver of control animals neither nuclei condensation nor chromatin fragmentation was detected. Occasionally, mitotic hepatocytes were found (Fig. 1). However, in tissue preparations obtained from animals 20 h after NNM administration, a number of hepatocytes showed condensed and fragmented chromatin characteristic for different stages of apoptosis (Fig. 1).

Secondly, the morphology of hepatocytes in H&E stained liver sections was examined. At 20 h after NNM administration morphological changes such as nuclei condensation and chromatin fragmentation were detected in about 5% of hepatocytes (Fig. 5B). Moreover, the fragmentation of DNA was determined by TUNEL assay. Sequential staining of the preparations with propidium iodide allowed to discriminate apoptotic from necrotic changes. Only TUNEL positive cells displaying concomitantly the chromatin condensation characteristic for apoptosis were scored. At 20 h after NNM administration DNA fragmentation was detected in about 5% of hepatocytes (Table II). This result correlates very well with the frequency of the apoptotic hepatocytes.

Depolarization of Mitochondria in Livers of NNM Treated Rats

The changes of the potential of the mitochondrial membrane induced by a variety of stress stimuli result in the release of distinct proteins into the cytoplasm [Daugas et al., 2000; Joza et al., 2001]. To assess the effect of NNM treatment on the status of the mitochondrial membrane, we determined the levels of cytochrome C and AIF in the cytoplasm (Fig. 2). Since NNM is a strong hepatocarcinogen, it would be expected that its genotoxic potential should be detected primarily in the target organ and in lower extent, if any, in other tissues. Crude PNS prepared from liver or testes homogenate was

TABLE I. Loss of the Liver Mass (g) After *N*-nitrosomorpholine (NNM) Treatment

	Animal no.						
Time after NNM (in h)	1	2	3	4	5	Mean	%
Control	3.43	3.42	4.00	3.85	ND	3.68	100.00
20	2.72	2.81	2.47	2.03	2.20	2.45	66.47
30	1.48	1.83	1.56	ND	ND	1.62	44.11
40	1.73	1.28	1.39	ND	ND	1.47	39.86

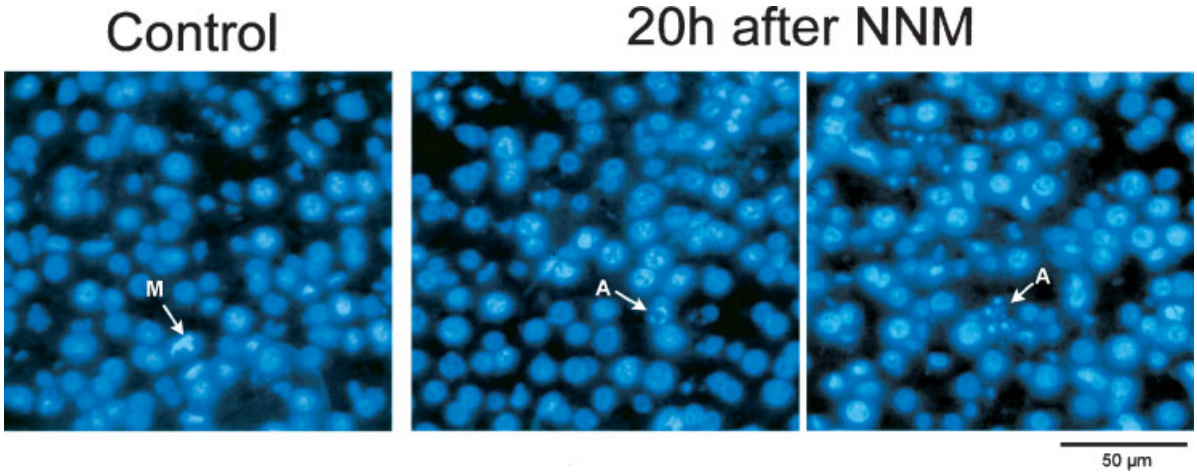

Fig. 1. Chromatin fragmentation in hepatocytes of rats treated with *N*-nitrosomorpholine (NNM). Tissue sections prepared from formaldehyde fixed liver specimens from control and rat at 20 h after NNM administration were stained with Hoechst. The mitotic (M) and apoptotic (A) cells are indicated by arrows.

further fractionated according to the method described by Fiskum et al. [2000]. During the ultracentrifugation step mitochondria were pelleted yielding a supernatant which was designated as a S-100 fraction. The analysis of S-100 samples revealed the increased accumulation of cytochrome C in the hepatocyte cytoplasma obtained from all rats at 20 and 30 h after NNM. The intensity of the cytochrome C band at 20 and 30 h was similar. Interestingly, the release of AIF from mitochondria showed slightly different kinetics. At 20 h a weak AIF signal especially in samples obtained from animals no. 1, 2, and 5 was observed. At 30 h post-treatment the cytoplasmic concentration of AIH increased as compared to that at 20 h. This observation is consistent with our previous results showing the delayed translocation of AIF protein as compared to that of cytochrome C [Tudzarova-Trajkovska and Wesierska-Gadek, 2003]. The analysis of S-100 samples isolated from testes revealed quite different results. No release of AIF from mitochondria could be detected at 20 and 30 h post-treatment. Whole cell lysate (WCL) from HeLa cells loaded as a control gave positive reaction in the blot thereby additionally substantiating that the lack of signal for AIF protein in testes samples was specific. However, S-100 fraction obtained from testes generated cytochrome C positive signals not only in samples prepared at 20 and 30 h after NNM administration but also in control rats. This result is contradictory to a number of other findings showing that in testes no stress response occurred within 30 h after NNM administration. Considering the fact that the anti-cytochrome C antibody strongly cross reacts in a number of cells and tissues with a protein band at about 70 kDa, we can not exclude that this antibody has a cross reactivity to an unknown protein at about 15 kDa strongly expressed in testes.

TABLE II. Fragmentation of DNA in Hepatocytes After NNM Treatment

Time after NNM (in h)	TdT-dUTP-nick-end-labeling (TUNEL) positive nuclei showing apoptotic morphology	
	%	fold of control
Control	0.3	1.0
12	3.0	10.0
20	4.9	16.3
40	4.0	13.3

PARP-1 Cleavage as a Marker of Targeting of Nuclear Proteins During Apoptosis

Our previous results [Wesierska-Gadek et al., 1999] showed a correlation between an onset of PARP-1 cleavage and induction of apoptosis after NNM treatment in rat liver. First, the generation of proteolytic fragments of PARP-1 in liver nuclei was detected already 6 h after NNM administration. At this time point the rate of apoptosis as evaluated on basis of morphological features or DNA fragmentation only slightly increased. Furthermore, in contrast to a series of heterogeneous fragments of human PARP-1 appearing after limited proteolysis [Wesierska-Gadek et al., 1999], in the liver of

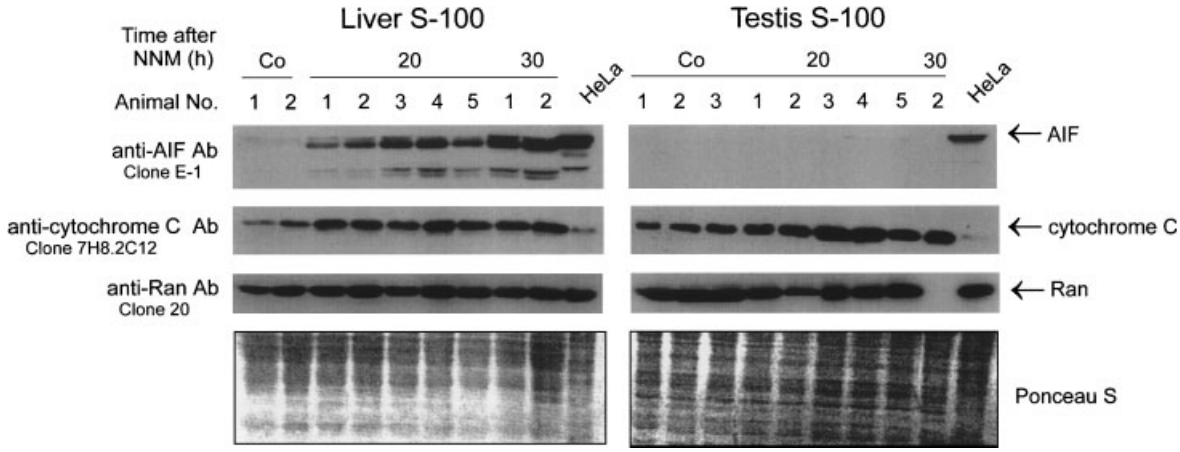

Fig. 2. Accumulation of apoptosis inducing factor (AIF) and cytochrome C in rat liver cytosol after NNM treatment. Proteins of S-100 fraction from liver and testes (30 μg protein/lane) were separated on 10% (AIF) and on 15% (cytochrome C) SDS slab gels. Whole cell lysate (WCL) from HeLa cells after treatment for 15 h with 40 μM cisplatin (CP) were loaded as a positive control. Equal protein loading was confirmed by Ponceau S staining of the blots and by sequential incubation with anti-ran antibodies. On 10% gel shown in the **right panel** (AIF and ran) molecular weight marker was loaded instead the sample at 30 h.

NNM treated rats two distinct degradation products lacking the N-terminal part were generated: one at 64 kDa and, in some samples an additional one at 54 kDa. The quantification by densitometry of the intensity of full-length protein signal visualized by the monoclonal anti-PARP antibody C-2-10 revealed a reduction of the intensity of the band representing intact PARP-1 by up to 40% in nuclei of NNM treated rats [Tudzarova-Trajkovska and Wesierska-Gadek, 2003]. Monitoring of PARP-1 status in the present study reproduced and largely extended former results. Interestingly, at 40 h post-treatment instead of the 64 kDa COOH-terminal polypeptide, a prominent band at 85 kDa appeared. The position of the 85 kDa fragment coincided with the canonical PARP-1 cleavage product generated by activated caspase-3 during p53 induced apoptosis in the human Ewing tumor cell line [Kovar et al., 2000] (Fig. 3A).

Onset of the Caspase-3 Mediated PARP-1 Cleavage in Hepatocytes at 20 h After NNM Administration

Appearance of the changed PARP-1 degradation pattern at 40 h post-treatment in the first experimental series inspired us to perform detailed analysis of samples isolated from distinct animals within the experimental groups. In the second experimental series at 16 h after NNM in none of the liver samples obtained from three animals the 85 kDa fragment of PARP-1 could be detected (Fig. 3B). However, after another 4 h the caspase-3 generated PARP-1 fragment appeared in liver samples (Fig. 3B). Comparison of the pattern of the cleaved PARP-1 generated between 20 and 40 h post-treatment revealed differences between distinct animals within the same treatment groups. In the experimental group at 20 h after NNM administration the 85 kDa PARP-1 fragment was detected in samples isolated from four of five animals. At 30 h the caspase-3 induced fragmentation of PARP occurred in all of three examined rats and at 40 h post-treatment in one of three rats. The detailed results obtained in two independent experimental series are summarized in Table III. Interestingly, careful inspection of the immunoblots shows that the intensity of the p85 kDa fragment of PARP-1 at the same experimental group largely varied indicating that the extent of PARP-1 cleavage may depend on the caspase-3 activity.

In testis, which is not a primary target of NNM toxicity, immunoblotting revealed only a single band at 116 kDa representing full-length enzyme (Fig. 3C) thereby confirming previous observations [Wesierska-Gadek et al., 1999] that cleavage of PARP-1 did not occur in this tissue after NNM administration.

Strong Activation of Effector Caspases Coincides With the Generation of the p85 PARP-1 Fragment

The generation of a 85 kDa fragment of PARP-1 appearing at 20 h and more pronounced at 30 and 40 h post-treatment strongly indicated

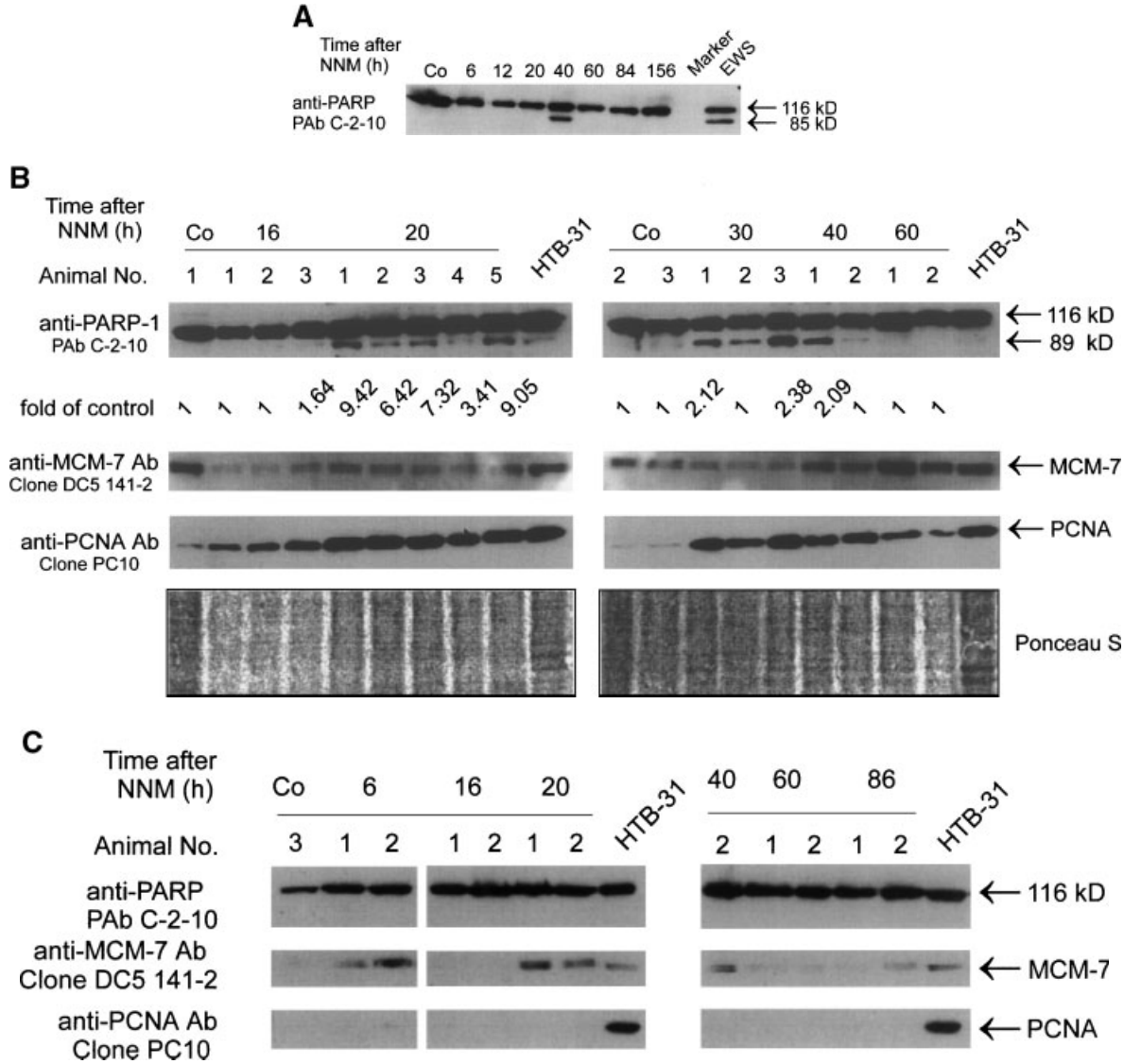

Fig. 3. Onset of generation of p85 poly(ADP-ribose) polymerase 1 (PARP-1) fragment in the liver at 20 h after NNM administration. **A**: The appearance of the p85 fragment of PARP-1 in liver nuclei isolated from rat at 40 h post-treatment. Proteins of nuclei isolated from rat liver (20 μg/lane) (1st experimental series) separated on 10% SDS gel were incubated with the monoclonal anti-PARP-1 C-2-10 antibody at a dilution of 1:3,000. The C-2-10 antibody reacts with the full-length enzyme as well as with its carboxy-terminal cleavage products but does not recognize the amino-terminal fragments generated by effector caspases. The intensity of full-length PARP-1 was quantified by densitometry. At 6 and 12 h post-treatment a reduction of the PARP-1 intensity by about 40 and 50%, respectively, was observed. A cell lysate of the human Ewing tumor cell line (EWS) expressing temperature-sensitive (ts) $p53^{138val}$ mutant was loaded as a positive control of caspase-3 generated PARP-1 cleavage. In this cell line activated caspase-3 cleaved PARP-1 during execution of apoptosis [Kovar et al., 2000]. **B**: Onset of PARP-1 degradation to 85 kDa product in the liver at 20 h post-treatment. Samples of liver nuclear proteins (2nd experimental series) from individual animals (30 μg protein/lane) within the experimental groups were simultaneously analysed on 10% SDS gels. Blots were first incubated with anti-PARP-1 C-2-10 monoclonal antibody and sequentially with anti-minichromosome maintenance-7 (MCM-7) and anti-PCNA antibodies. Equal protein loading was confirmed by Ponceau S staining of the blots. Total cell lysate prepared from human cervix carcinoma HTB-31 cells was loaded as a full-length PARP-1 positive control. The intensity of p85 product was quantified by densitometry. **C**: Lack of PARP-1 degradation in nuclei isolated from testis. Analyzed samples were from 2nd experimental series. Conditions of the analysis as in Figure 3B.

that the effector caspases have been activated. To assess the activation of caspase-3, we performed two different approaches. In the first approach, the activation of caspase-3 was examined by immunoblotting. Since caspases are acting primarily in cytoplasm, we analyzed proteins of PNSs obtained during subfractionation of rat liver samples from control animals

TABLE III. Frequency of the Presence of the p85 Poly(ADP-Ribose) Polymerase 1 (PARP-1) Fragment in Rat Liver Nuclei After NNM Treatment

Liver nuclei							
Control		20 h after NNM		30 h after NNM		40 h after NNM	
1st exp.	2nd exp.	1st exp.	2nd exp.	1st exp.	2nd exp.	1st exp.	2nd exp.
0/3	0/3	1/3	4/5	ND	3/3	2/3	1/3
		4/8		3/3		3/6	
		50%		100%		50%	
				10/17 (60%)			

and rats exposed to NNM. As shown in Figure 4A in liver samples obtained from control animals only the pro-zymogen form was detected. At 30 h after NNM administration a p17 band representing the large subunit of activated caspase-3 was detected in samples obtained from two distinct animals. The activation of caspase-3 followed temporally that of caspase-9 [Tudzarova-Trajkovska and Wesierska-Gadek, 2003] and coincided with the generation of a strong band at 85 kDa representing the canonical fragment of PARP-1.

The analysis of the cytosolic proteins prepared from testes of the same animals revealed only the presence of the inactive pro-zymogen form (not shown).

In the second approach the activity of caspase-3/7 was quantified. The basal activity of caspase-3/7 in the liver of control rats was very low (about 11,000 cpm/μg protein). As depicted in Figure 4B the activity of liver caspase-3/7 increased about 5-fold and 25-fold at 20 and 30 h post-treatment, respectively. The increase was statistically significant. At 40 h the caspase-3 activity remained elevated (not shown). However, in testes no or very slight augmentation of caspase-3/7 activity occurred at 20 and 30 h, respectively.

These results strongly correlate with the onset of the generation of the p85 fragment of PARP-1 in rat liver but not in testis.

Extent of Caspase-3 Activation Differs Between Individual Animals

The extent of caspase-3 activation in individual animals in the experimental groups examined at 20 and 30 h after NNM administration was additionally compared. The activity of caspases 3/7 in rat liver at 20 h differed between individual rats (Fig. 4C). The high activity values measured in rats nos. 1 and 5 coincided with the stronger intensity of the p85 kDa band detected by immunoblotting (Fig. 3B). However, this correlation was not observed in all animals indicating that the execution of apoptosis in vivo is a more complex process. The above data reflect very well the differences in the extent of the activation of apoptotic effectors among individual animals.

Detection of Caspase-3 Mediated PARP-1 Fragmentation Solely in Hepatocytes Undergoing Apoptosis

To further assess a link between the induction of apoptosis and caspase-3 mediated PARP-1 cleavage, we performed immunostaining of the liver sections using antibodies recognizing exclusively PARP-1 cleaved at position 214/215. The DEVD tetrapeptide representing the motif most specifically targeted by activated caspase-3 is harbored in the PARP-1 molecule from aa 212to aa 215. To ensure that the anti-p85 antibody does not cross-react with the full-length PARP-1, we tested its reactivity with human cervical carcinoma HeLa cells undergoing apoptosis after treatment with DOX and CP [Wesierska-Gadek et al., 2002]. The anti-p85 antibody generated against a chemically synthesized peptide corresponding to the cleavage site of PARP-1 (214/215) was purified from rabbit serum by sequential epitope-specific chromatography. As shown in Figure 5A the antibody did not recognize full-length PARP-1 in cell lysate prepared from control and apoptotic HeLa cells as evidenced by immunoblotting. Furthermore, the anti-p85 antibody failed to stain the nuclei in untreated control cells (Fig. 5A). In the population of control cells no apoptotic cells were found as evidenced by 4,6-diamidino-2-phenylindole (DAPI) staining. However, this antibody strongly stained a p85 cleavage product of PARP-1 appearing in cell

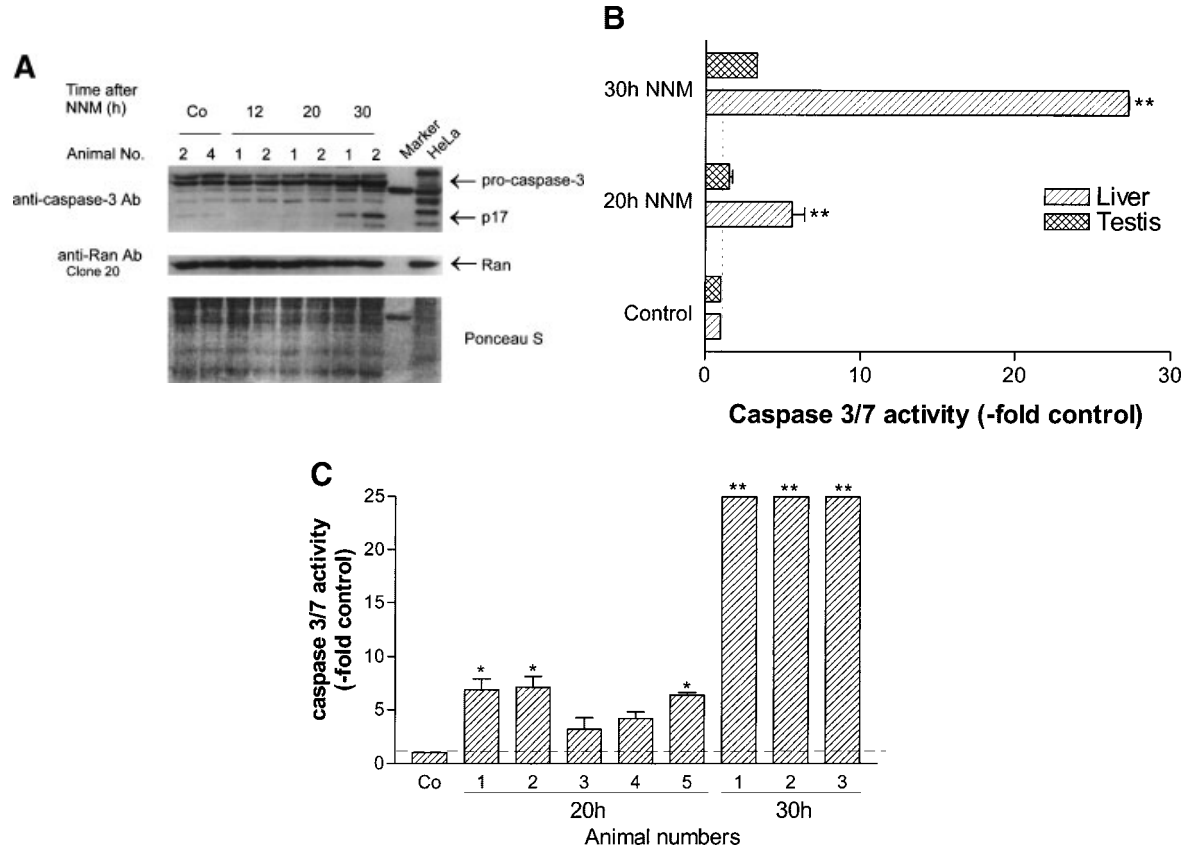

Fig. 4. Activation of caspase-3 in rat hepatocytes in vivo 20 h after NNM treatment. **A**: Detection of activated caspase-3 by immunoblotting. Proteins of S-100 fraction (30 μg protein/lane) were loaded on 15% SDS gel. Immunoblot was performed with polyclonal anti-caspase-3 antibodies (Upstate). Carbonic anhydrase (30 kDa) was loaded as a molecular weight marker. WCL from HeLa cells treated for 15 h with 40 μM CP was loaded as a positive control. Equal protein loading was confirmed by Ponceau S staining of the blot and by sequential incubation with anti-ran antibodies. **B**: A strong activation of caspase-3/7 in the liver beginning at 20 h after NNM administration. Caspase-3/7 activity was determined quantitatively using APO-One Caspase-3/7 Assay (Promega). Proteins of S-100 fraction (5 μg protein/tube) diluted with phosphate-buffered saline (PBS) to a final volume of 50 μl were mixed with caspases substrate Z-DEVD-R110. After incubation for 2, 4, and 20 h at 37°C, fluorescence was measured at 485 nm. Sucrose solution was used as a blank. Four replicates of each sample were measured. Assay was repeated four times. The graph was generated from values measured after 4 h incubation. Statistical significance was determined using the ANOVA test followed by Dunnett's Multiple Comparison test (all treatment groups vs. corresponding control). Bars indicate mean ± SD. Asterisks indicate statistical significance valuated with ANOVA test: $^{**}P < 0.01$; $^{*}P < 0.05$. **C**: Variability of liver caspase-3/7 activity between individual animals within the same experimental group. Conditions of the determination and evaluation as in Figure 4B.

lysates after treatment with DOX or with etoposide (Fig. 5A). Sequential incubation of the blot with the monoclonal anti-PARP-1 antibody C-2-10 visualized additionally the band representing full-length PARP-1 thereby evidencing the presence of the intact enzyme. However, the intensity of the caspase-cleavaged PARP-1 band stained by antibody C-2-10 was largely weaker than that stained by anti-p85 antibody. The PARP-1 cleavage after 6 h DOX was poorly detectable by C-2-10 antibody. In preparations of cells treated for 14 h with 20 μM CP or with 1 μM DOX, nuclei at different stages of apoptosis stained strongly for p85. The changes characteristic for apoptosis such as chromatin condensation and nuclear fragmentation were visualized by DAPI staining. A close correlation between chromatin fragmentation and positive staining for p85 was observed. On the other hand, the antibody directed against full-length PARP-1 stained all nuclei (not shown). These detailed tests confirmed the high specificity and selectivity of the anti-p85 antibody.

In tissue sections prepared from control rats no p85 signal could be detected. However, the immunohistochemical staining of the liver sections obtained from rats at 20 h after NNM

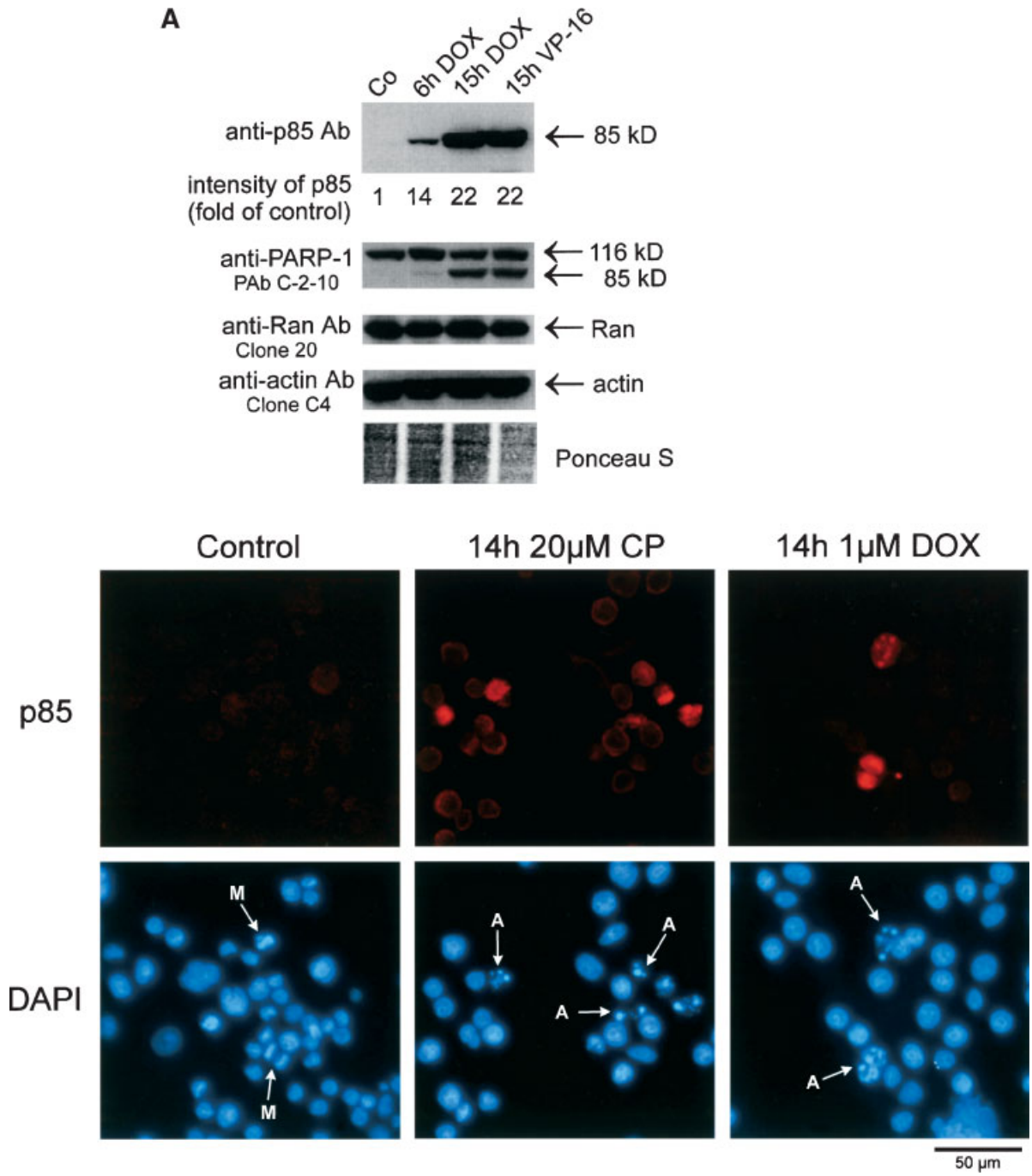

Fig. 5. Detection of p85 PARP-1 fragment exclusively in hepatocytes undergoing apoptosis. **A**: Specificity of anti-p85 antibody for cells in different stages of apoptosis. Human cervix carcinoma HeLa cells were treated with distinct anti-cancer drugs [1 μM doxorubicin (DOX), 20 μM CP, or with 10 μM etoposide (VP-16)] for indicated periods of time. Then controls and drug-treated cells were lysed or fixed with 4% paraformaldehyde. WCLs (**upper panel**) were analyzed by immunoblotting. The blot was probed with anti-p85 antibody (Promega) recognizing exclusively caspase-3 cleaved PARP-1 fragment at 85kDa and sequentially with monoclonal anti-PARP-1 antibody C-2-10. The equal loading was confirmed by sequential incubation with anti-ran and anti-actin antibodies. Paraformaldehyde fixed cells (**lower panel**) were stained with the anti-p85 antibody according to the manufacturer's protocol. The immune complexes were visualized using secondary antibodies coupled to Cy-3 (Amersham International). Nuclei were stained with DAPI. Images were performed using Nikon digital camera. **B**: Detection of p85 PARP-1 fragment in hepatocytes undergoing apoptosis at 20 h post-treatment. Mitotic hepatocytes (M) and hepatocytes undergoing apoptosis (A) are indicated by arrows. **C**: p85 PARP-1 fragment staining in hepatocytes at different stages of apoptosis. C—**upper panels**, lower magnification; **lower panels**, higher magnification. Hepatocytes at different stages of apoptosis (A) are indicated by arrows. **D**: Global positive signals for full-length PARP-1 in liver nuclei.

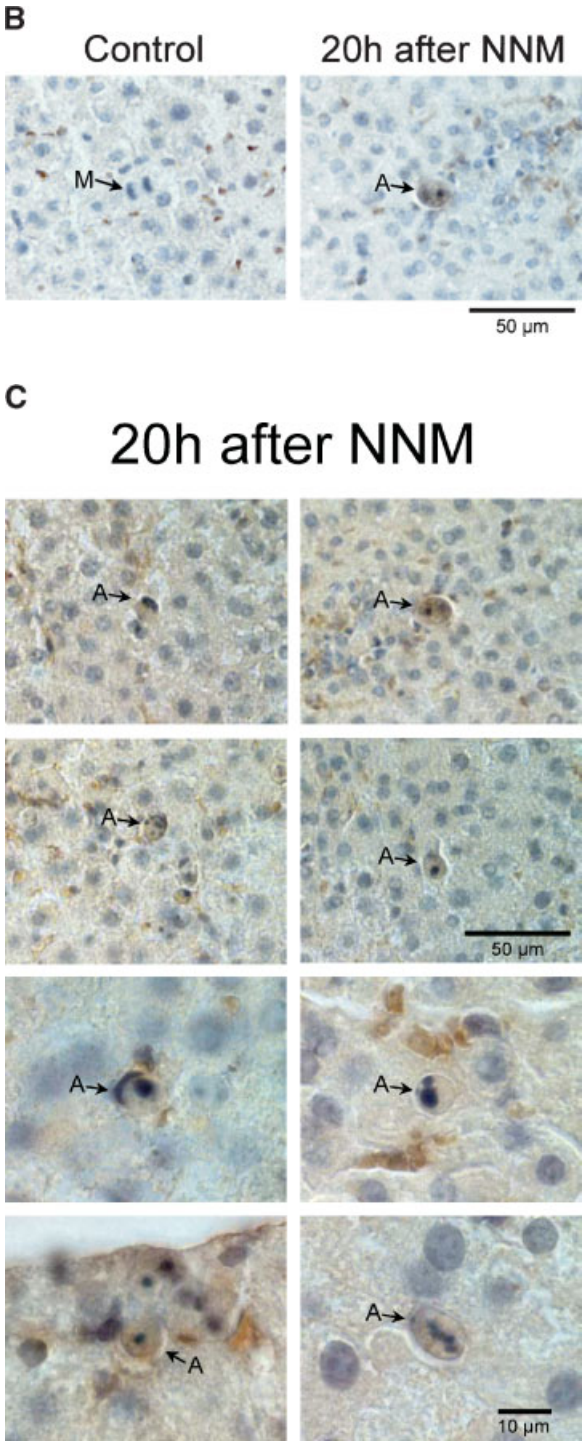

Fig. 5. (*Continued*)

revealed the presence of p85 signals in a number of hepatocytes at different stages of apoptosis (Fig. 5B,C). Only hepatocytes exhibiting the features of apoptosis were stained. The specificity of this reactivity was additionally confirmed by immunostaining with an antibody against full-length PARP-1 (Fig. 5D). In contrast to the other antibody, the polyclonal antibody directed against full-length PARP-1 stained all hepatocytes in tissue sections from control rats as well as from rats at 20 h post-treatment.

PCNA Increase in Liver of NNM Treated Rats

It is known that in adult rat liver the DNA synthesis is reduced to a barely detectable level and hepatocytes are largely in G_0 phase of the cell cycle. As expected, PCNA was hardly detectable in the nuclei isolated from rat liver of control animals (Fig. 3B). However, 20 h after NNM administration a strong upregulation of PCNA concentration was observed. The high PCNA expression in the liver nuclei persisted for further 20 and at 60 h post-treatment PCNA levels decreased. On the other hand, the levels of MCM-7 protein at 20 and 40 h were moderate. Monitoring of the levels of MCM-7 protein has been reported to be suitable for discrimination between cells maintained in the G_0 or G_1 phase of the cell cycle [Labib et al., 2001]. MCM-7 is expressed in cells G_1 phase. However, in cells resting in the G_0 phase, MCM-7 messenger RNA and MCM-7 protein are downregulated. In control rats MCM-7 was detected in the liver nuclei but not in the nuclei isolated from testes indicating in the latter tissue cells were arrested in G_0 phase. Remarkably, no PCNA signals could be detected in the nuclei prepared from testes (Fig. 3C). These data together indicate that the increase of PCNA in rat liver is attributable to the induction of DNA repair [Shivji et al., 1992]. This observation is in concordance with our recent data [Tudzarova-Trajkovska and Wesierska-Gadek, 2003].

DISCUSSION

PARP-1 recognized a couple of years ago as an early and very specific nuclear target for effector caspases was acknowledged as a very useful marker for monitoring of the progression of apoptosis [Kaufmann et al., 1993; Lazebnik et al., 1994]. However, recently published data attest PARP-1 more and more an active role in the regulation of apoptosis in response to a variety of stress stimuli [Chiarugi and Moskovitz, 2002; Yu et al., 2002].

PARP-1, the most abundant enzyme catalyzing formation of poly(ADP-ribose) chains in mammalian cells is highly activated by DNA strand breaks generated directly by agents

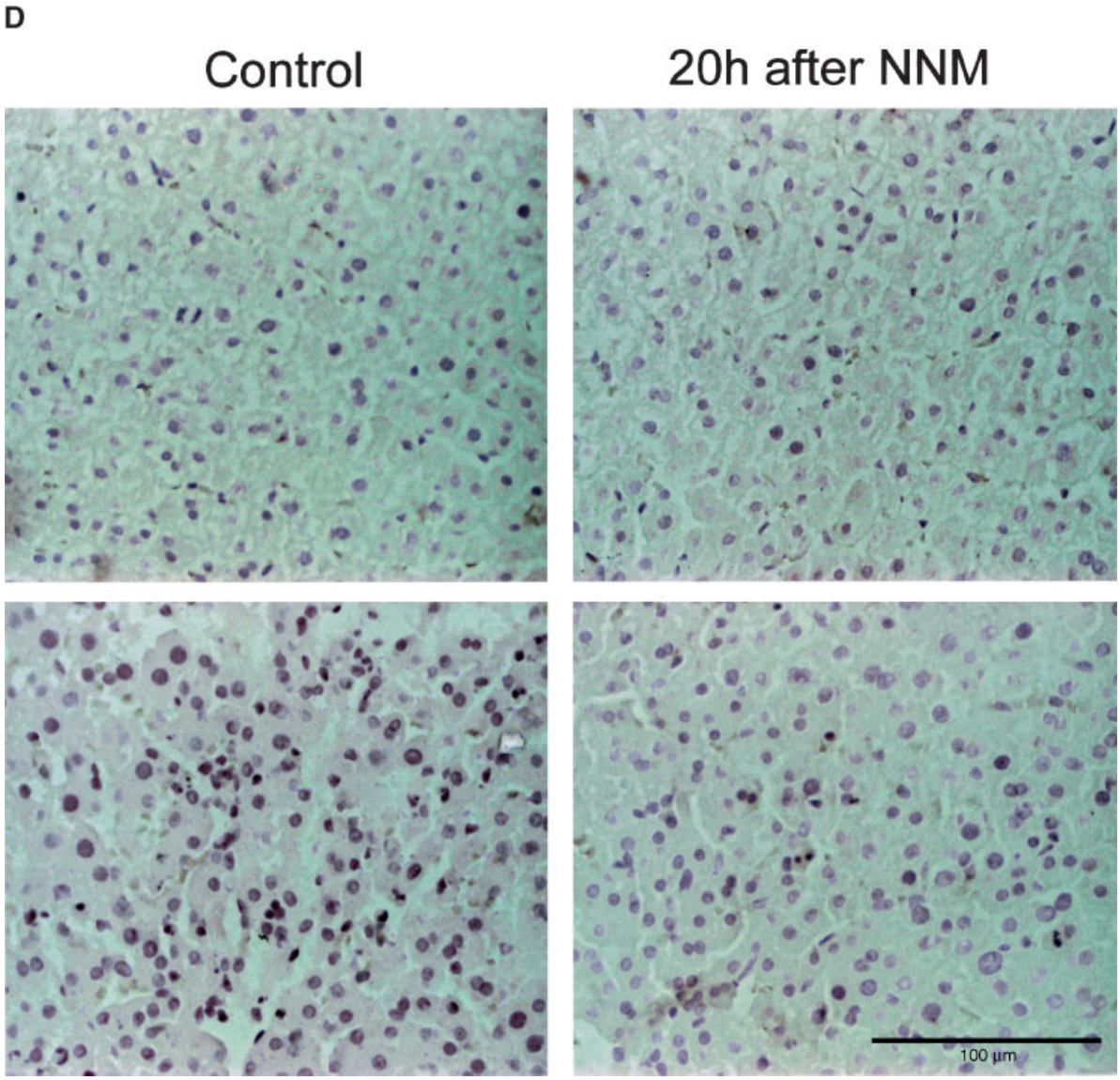

Fig. 5. (*Continued*)

affecting the integrity of DNA or indirectly by different types of stress [for review, see D'Amours et al., 1999]. The rapid synthesis of poly(ADP-ribose) chains by stimulated PARP-1 leads to enhanced consumption of its substrate NAD+ and as a consequence to its exhaustion. The total depletion of cellular energy stores, especially compartmentalized within mitochondria results in the depolarization of the mitochondrial membrane and mitochondrial dysfunction [Chiarugi, 2002]. Recently, the active involvement of PARP-1 in the regulation of apoptosis has been identified [Chiarugi and Moskovitz, 2002; Yu et al., 2002]. The depletion of cellular energy followed by mitochondrial injury and subsequent AIF release and nuclear translocation initiated the programmed cell death [Yu et al., 2002]. It has also been shown that pharmacological or genetic inactivation of PARP-1 during conditions of cellular stress is beneficial. The caspase-3 mediated cleavage of PARP-1 occurring during execution of apoptosis separates the DNA-binding and catalytic domain thereby inactivating the cellular enzyme. Therefore, the elimination of PARP-1 activity in distinct cells by a single cut introduced by effector caspases seems to be more selective than the global inhibition after administration of pharmacological agents and could be locally beneficial for target tissues. One could speculate

that elimination of PARP-1 activity by its cleavage would protect affected tissues from secondary effects [Chiarugi, 2002].

Considering the essential role of PARP-1 in the regulation of programmed cell death, we performed a detailed analysis of the kinetics of PARP-1 cleavage in vivo during NNM induced apoptosis and compared it with that of caspases-3 activation.

There is only few data on the processing of PARP-1 in the liver during apoptosis in vivo. Some of them are inconsistent. We have observed early degradation of PARP-1 to 64 and 54 kDa peptides in vivo in liver but not in testes of rats after administration of NNM [Wesierska-Gadek et al., 1999]. The appearance of degradation products coincided with the reduction of the full-length enzyme. Both fragments at 64 and at 54 kDa failed to react with the anti-PARP-1 antibody N-20 recognizing an epitope within the first 20 amino acids of the enzyme thereby indicating that they lacked the amino-terminus [Wesierska-Gadek et al., 1999]. On the other hand the 64 kDa PARP-1 bound ^{32}P-labeled NAD+ thereby evidencing the presence of the substrate binding domain which is localized within the carboxy-terminus of PARP-1 [Wesierska-Gadek et al., 1999]. The size of the 64 kDa PARP-1 fragment coincided with that generated by granzyme B. Recently, the nuclear accumulation of granzym B was detected at early times after administration of NNM [Tudzarova-Trajkovska and Wesierska-Gadek, 2003]. This observation implicates that proteolytic degradation of PARP-1 to 64 kDa could be mediated by granzym B [Froelich et al., 1996]. Surprisingly, at 40h post-treatment instead of the 64/54 kDa fragments a 85 kDa cleavage product of PARP-1 appeared [Tudzarova-Trajkovska and Wesierska-Gadek, 2003] strongly indicating that it was generated by activated caspase-3. On the other hand, the resistance of PARP-1 in the liver to caspase-3 has been reported [Jones et al., 1999]. To clarify this inconsistency, we performed a detailed analysis of the proteolytic processing of PARP-1 in vivo. We examined samples isolated from two distinct tissues from the same animals, liver and testes. We determined the kinetics of the appearance of the p85 PARP-1 fragment with that of caspases-3 activation. Moreover, we analyzed the caspases-3 activity and intensity of the p85 fragment in tissue samples prepared from individual animals. The detailed analysis of liver samples revealed that the activation of caspases-3 coincided temporally with the generation of the p85 PARP-1 fragment and release of AIF from mitochondria due to loss of the membrane potential. The maximal activation of effector caspases was observed at 30 and 40 h post-treatment. At 60 h after NNM administration the p85 band disappeared. The p85 PARP-1 cleavage was detected exclusively in hepatocytes undergoing apoptosis. The intensity of the p85 fragment correlated, at least partially, with the extent of caspases-3 activation. In testes, neither activation of caspases-3 nor of p85 fragment could be detected evidencing that NNM as the strong hepatocarcinogen primarily affected the target organ.

Our present results show that PARP-1 is cleaved in liver by activated caspase-3. A close correlation between appearance of the p85 fragment and the activation of caspase-3 was evidenced. Not only the general kinetics of the increase of caspase-3 activity coincided with the onset of generation of p85 degradation product but also inter-individual differences between distinct animals.

Thus, our detailed study unequivocally evidences the susceptibility of nuclear PARP-1 in liver to caspase-3 mediated cleavage. However, it cannot be excluded that the processing of PARP-1 in isolated hepatocytes exposed to the same insults would differ from that observed in vivo. Our preliminary data from experiments performed on primary rat hepatocytes cultivated for 24 h confirm this assumption. Treatment of hepatocytes with NNM in the cell culture failed to induce caspases-3 mediated PARP-1 cleavage (our unpublished data). This observations could be explained by the requirement to activate the carcinogen in vivo [Manson et al., 1978]. Moreover, one cannot exclude that a cooperation between different types of cells, e.g., Kupfer cells and hepatocytes is necessary for signal transduction.

ACKNOWLEDGMENTS

The authors thank Dr. W. Mosgoeller for preparation of tissue sections.

REFERENCES

Brambilla G, Carlo P, Finollo R, Sciaba L. 1987. Dose-response curves for DNA fragmentation induced in rats by sixteen *N*-nitroso compounds as measured by viscometric and alkaline elution analyses. Cancer Res 47: 3485–3491.

Chiarugi A. 2002. Poly(ADP-ribose) polymerase: Killer or conspirator? The "suicide hypothesis" revisited. Trends Pharmacol Sci 23:122–129.

Chiarugi A, Moskovitz MA. 2002. PARP-1—A perpetrator of apoptotic cell death? Science 297:200–201.

D'Amours D, Desnoyers S, D'Silva I, Poirier GG. 1999. Poly(ADP-risyl)ation reactions in the regulation of nuclear function. Biochem J 342:249–268.

Daugas E, Nochy D, Ravagnan L, Loeffler M, Susin SA, Zamzami N, Kroemer G. 2000. Apoptosis-inducing factor (AIF): A ubiquitous mitochondrial oxidoreductase involved in apoptosis. FEBS Lett 476:118–123.

Enzmann H, Bannasch P. 1987. Morphometric study of alterations of extrafocal hepatocytes of rat liver treated with *N*-nitrosomorpholine. Virchows Arch B Cell Pathol Incl Mol Pathol 53:218–226.

Fiskum G, Kowaltowksi AJ, Andreyev AY, Kushnareva YE, Starkov AA. 2000. Apoptosis-related activities measured with isolated mitochondria and digitonin-permeabilized cells. Methods Enzymol 322:222–234.

Froelich CJ, Hanna WL, Poirier GG, Duriez PJ, D'Amours D, Salvesen GS, Alnemri ES, Earnshaw WC, Shah GM. 1996. Granzyme B/perforin mediated apoptosis of Jurkat cells results in cleavage of poly(ADP-ribose) polymerase to the 89-kDa apoptotic fragment and less abundant 64-kDA fragment. Biochem Biophys Res Commun 227: 658–665.

Jones RA, Johnson VL, Hinton RH, Poirier GG, Chow SC, Kass GEN. 1999. Liver poly(ADP-ribose)polymerase is resistant to cleavage by caspases. Biochem Biophys Res Commun 256:436–441.

Joza N, Susin SA, Daugas E, Stanford WL, Cho SK, Li CY, Sasaki T, Elia AJ, Cheng HY, Ravagnan L, Ferri KF, Zamzami N, Wakeham A, Hakem R, Yoshida H, Kong YY, Mak TW, Zuniga-Pflucker JC, Kroemer G, Penninger JM. 2001. Essential role of the mitochondrial apoptosis-inducing factor in programmed cell death. Nature 410:549–554.

Kaufmann SH, Desnoyers S, Ottaviano Y, Davidson NE, Poirier GG. 1993. Specific proteolytic cleavage of poly-(ADP-ribose)polymerase: An early marker of chemotherapy-induced apoptosis. Cancer Res 53:3976–3985.

Kovar H, Jug G, Printz D, Schmid G, Wesierska-Gadek J. 2000. Characterization of distinct consecutive phases in non-genotoxic p53-induced apoptosis of Ewing tumor cells and the rate-limiting role of caspase 8. Oncogene 19:4096–4107.

Labib K, Kearsey SE, Diffley JF. 2001. MCM2-7 proteins are essential components of prereplicative complexes that accumulate cooperatively in the nucleus during G_1-phase and are required to establish, but not maintain, the S-phase checkpoint. Mol Biol Cell 12:3658–3667.

Lazebnik YA, Kaufmann SH, Desnoyers S, Poirier GG, Earnshaw WC. 1994. Cleavage of poly(ADP-ribose) polymerase by a proteinase with properties like ICE. Nature 371:346–347.

Manson D, Cox PJ, Jarman M. 1978. Metabolism of *N*-nitrosomorpholine by the rat in vivo and by rat liver microsomes and its oxidation by the Fenton system. Chem Biol Interact 20:341–354.

Moore MA, Mayer D, Bannasch P. 1982. The dose dependence and sequential appearance of putative preneoplastic populations induced in the rat liver by stop experiments with *N*-nitrosomorpholine. Carcinogenesis 3:1429–1436.

Shivji MKK, Kenny MK, Wood RD. 1992. Proliferating cell nuclear antigen is required for DNA excision repair. Cell 69:367–374.

Stewart BW, Hicks RM, Magee PN. 1975. Acute biochemical and morphological effects of *N*-nitrosomorpholine in comparison to dimethyl- and diethylnitrosamine. Chem Biol Interact 11:413–429.

Tamm I, Schriever F, Doerken B. 2001. Apoptosis: Implications of basic research for clinical oncology. Lancet Oncol 2:33–42.

Tata JR. 1974. Isolation of nuclei from rat liver and other tissues. Methods Enzymol 31:253–262.

Thorgeirsson SS, Teramoto T, Factor VM. 1998. Dysregulation of apoptosis in hepatocellular carcinoma. Semin Liver Dis 18:115–122.

Tudzarova-Trajkovska S, Wesierska-Gadek J. 2003. Strong induction of p73 protein in vivo coincides with the onset of apoptosis in rat liver after treatment with the hepatocarcinogen *N*-nitrosomorpholine (NNM). L Cell Biochem 90:837–855.

Weber E, Bannasch P. 1994. Dose and time dependence of the cellular phenotype in rat hepatic preneoplasia and neoplasia induced by continuous oral exposure to *N*-nitrosomorpholine. Carcinogenesis 15:1235–1242.

Wesierska-Gadek J, Grimm R, Hitchman E, Penner E. 1998. Members of the glutathione *S*-transferase gene family are antigens in autoimmune hepatitis. Gastroenterology 114:329–335.

Wesierska-Gadek J, Bugajska-Schretter A, Löw-Baselli A, Grasl-Kraupp B. 1999. Cleavage of poly(ADP-ribose) transferase during p53-independent apoptosis in rat liver after treatment with *N*-nitrosomorpholine and cyproterone acetat. Mol Carcinog 24:263–275.

Wesierska-Gadek J, Schloffer D, Kotala V, Horky M. 2002. Escape of p53 protein from E6-mediated degradation in HeLa cells after cisplatin therapy. Int J Cancer 101: 128–136.

Yu S-W, Wang H, Poitras MF, Coombs C, Bowers WJ, Fereroff HJ, Poirier GG, Dawson TM, Dawson VL. 2002. Mediation of poly(ADP-ribose) polymerase-1-dependent cell death by apoptosis-inducing factor. Science 297: 259–263.